RESEARCH ARTICLE

Molecular signaling operated by a diet-compatible mixture of oxysterols in up-regulating CD36 receptor in CD68 positive cells

Gabriella Leonarduzzi[1], Simona Gargiulo[1], Paola Gamba[1]*, Maria-Giulia Perrelli[1], Isabella Castellano[2], Anna Sapino[2], Barbara Sottero[1] and Giuseppe Poli[1]*

[1] Department of Clinical and Biological Sciences, University of Turin, San Luigi Hospital, Orbassano, Turin, Italy
[2] Department of Biomedical Sciences and Human Oncology, University of Turin, Turin, Italy

Received: October 9, 2009
Revised: November 9, 2009
Accepted: November 11, 2009

Oxidation of dietary cholesterol during food storage and processing, and/or that of endogenous cholesterol in the presence of increased steady-state levels of reactive oxygen species, leads to the production of derivatives, termed oxysterols. Among the biochemical effects exerted by an oxysterol mixture, it has recently been observed that marked up-regulation of CD36 scavenger receptor on macrophage cells plays a primary role in foam cell formation. This article reports evidence of a significant co-localization of CD36 receptor with cells of the macrophage lineage, *i.e.* CD68 positive cells, LDL apoprotein B100 and lipids in human advanced atherosclerotic lesions. In addition, it provides a comprehensive analysis of the molecular signaling operated by a nutritionally relevant mixture of oxysterols in overexpressing CD36 receptor in cells of the macrophage lineage. The involvement of a G protein, Src, phospholipase C cascade and peroxisome proliferator-activated receptor γ in oxysterol-mediated signaling was demonstrated by using selective inhibitors, while the central role of the downstream protein kinase Cδ and extracellular signal-regulated kinase pathways in oxysterol-induced enhancement of CD36 was conclusively proved by means of small interfering RNA (siRNA) technology.

Keywords:
Atherosclerosis / CD36 scavenger receptor / Cell signaling / Cholesterol / Oxysterols

1 Introduction

The contribution of dietary cholesterol to the pathogenesis of atherosclerosis has long been debated, but nowadays, on the basis of the accumulated bulk of experimental, epidemiological and clinical evidence, it may be assumed that cholesterol ingested in the diet at least contributes to sustaining and worsening the atherosclerotic process [1, 2]. With regard to the mechanism(s) by which cholesterol might favor the development of atherosclerosis, maximum consideration is given to inflammation [3], namely the main driving force of all major chronic disease processes occurring in humans. However, unoxidized cholesterol does not appear to exert *per se* a significant pro-inflammatory effect, while several oxysterols (27-carbon derivatives of cholesterol oxidation) of both dietary and endogenous origin are recognized to markedly enhance and sustain inflammation in the vascular wall [4–7].

The large majority of oxysterols of interest in pathophysiology are found in food and food derivatives: in particular, 7-ketocholesterol, 7α-hydroxycholesterol, 7β-hydroxychol-

Correspondence: Professor Giuseppe Poli, Department of Clinical and Biological Sciences, University of Turin, San Luigi Hospital, 10043 Orbassano, Turin, Italy
E-mail: giuseppe.poli@unito.it
Fax: +39-116705424

Abbreviations: ERK1/2, extracellular signal-regulated kinases 1 and 2; **MEK1/2,** mitogen-activated protein kinase/extracellular signal-regulated kinase kinases 1 and 2; **pERK,** phosphorylated extracellular signal-regulated kinase; **PKCδ,** protein kinase C δ; **PLC,** phospholipase C; **PPARγ,** peroxisome proliferator-activated receptor γ; **siRNA,** small interfering RNA

*These authors have contributed equally to this work.

© 2010 WILEY-VCH Verlag GmbH & Co. KGaA, Weinheim

esterol, 5α,6α-epoxycholesterol, 5β,6β-epoxycholesterol, cholestan-3β,5α,6β-triol and 25-hydroxycholesterol [8]. Further, and more importantly, several factors are known to accelerate the oxidation of food cholesterol: in particular, UV and γ-radiation, photo-oxidation, heat, the presence of oxygen and of pro-oxidant agents, and storage conditions [9, 10]. Oxidized cholesterol products are absorbed from the food and contribute to the pool of oxidized lipids in circulating lipoproteins [11].

A considerable accumulation of experimental data supports the strong inflammatory potential of cholesterol oxidation products [12]. In particular, an oxysterol mixture compatible with that detectable in human hypercholesterolemic plasma and including all major oxysterols of dietary origin has, in cells of the macrophage linage, been proved to markedly up-regulate expression and synthesis of the pro-inflammatory mediators transforming growth factor β1 [13] and monocyte chemotactic protein-1 [14].

Thus, oxidation of cholesterol definitely appears to be the molecular event that links hypercholesterolemia to atherosclerosis through the promotion of inflammatory reactions. Moreover, the atherogenic process implies a key role for monocytes/macrophages in foam cell formation and accumulation. Importantly, the same oxysterol mixture that was shown to recruit and stimulate macrophages can also induce a sustained increase in both expression and synthesis of CD36 scavenger receptor in the same cells [15]; this receptor is generally recognized as being essential in the generation of foam cells [16]. Indeed, oxysterol-treated macrophage cells rapidly turn into lipid-laden cells when incubated in the presence of oxidized LDL, a phenomenon that is fully prevented by cell pretreatment with anti-CD36 specific antibodies [15].

Following such key experimental evidence, a comprehensive and complete investigation of the molecular signaling by which oxysterols induce CD36 overexpression in cells of the macrophagic lineage was carried out. Moreover, it was also deemed of interest to simultaneously verify in advanced human carotid plaques the actual localization of macrophage cells (CD68 positive cells), CD36 receptors, LDL apoprotein B100 and LDL lipids. The findings obtained from these molecular and histochemical analyses are reported here.

2 Materials and methods

2.1 Human atherosclerotic plaques

The histochemical analysis was approved by the local ethical committee and all patients provided an informed consent. Ten atherosclerotic carotid plaques were obtained from patients with symptomatic high-grade internal carotid artery stenosis undergoing carotid endarterectomy.

2.2 Immunohistochemical detection of CD68, CD36 and apoprotein B100 in human carotid plaques

Sequential sections from frozen human carotid plaques were fixed in 4% formalin. The sections were incubated with mouse anti-human CD68 (1:50) (AbD Serotec, Oxford, UK) or anti-CD36 (1:10) (clone FA6-152, HyCult Biotechnology b.v., Huden, The Netherlands) or anti-apoprotein B100 (1:100) monoclonal antibodies overnight at 4°C. For immunohistochemical detection of CD68 and CD36 the sections were then incubated with an anti-mouse secondary antibody (1:200) (DakoCytomation, Milan, Italy) for 1 h and then with avidin-biotin complex (1:20) (DakoCytomation) for 30 min at room temperature. Finally, to reveal peroxidase activity, sections were incubated in freshly prepared 0.1% 3,3′-diaminobenzidine solution in the dark for 10 min and counterstained with Mayer's hematoxylin (Sigma-Aldrich, Milan, Italy). Thereafter, the plaque sections were mounted in DPX (Sigma-Aldrich), and observed under a light microscope. Images were acquired by the ''Leica DCF Twain'' program. For apoprotein B100 detection, the plaque sections were incubated with a goat anti-mouse FITC-conjugated secondary antibody (1:50) (DakoCytomation). Slides mounted with MOWIOL 4–88 (Calbiochem-Merck, Darmstadt, Germany) were observed under the LSM 510 confocal laser microscope (Carl Zeiss SpA, Arese, Milan, Italy).

2.3 Nile red staining of plaque sections

Frozen carotid plaque sections were stained with a fresh solution of Nile red (1:1000) (Sigma-Aldrich) in the dark at room temperature for 5 min. Sections, mounted in MOWIOL 4–88 (Calbiochem-Merck), were observed with a LSM 510 confocal laser microscopy system (Carl Zeiss SpA).

2.4 Cell culture and treatments

The human promonocytic cell line U937 was grown in RPMI-1640 (Lonza Milano Srl, Caravaggio, Italy) and dispensed as described elsewhere [14]. Cells (1×10^6/mL) were treated with the oxysterol mixture (20 μM) or with unoxidized cholesterol (20 μM) (Steraloids, Newport, RI, USA), both dissolved in ethanol, or with an equivalent volume of ethanol (12.5 mM) used as solvent control. The percentage composition of the oxysterol mixture used was 7α-hydroxycholesterol (5%), 7β-hydroxycholesterol (10%), 5α,6α-epoxycholesterol (20%), 5β,6β-epoxycholesterol (20%), cholestan-3β,5α,6β-triol (9%), 7-ketocholesterol (35%) and 25-hydroxycholesterol (1%).

For chemical inhibitor studies, cells were pre-treated with PP2 (2 μM), a tyrosine kinase c-Src inhibitor, or with U73122 (2 μM), a phospholipase C (PLC) inhibitor or with PD98059 (20 μM), a selective mitogen-activated protein kinase/extracellular signal-regulated kinase kinase 1/2

© 2010 WILEY-VCH Verlag GmbH & Co. KGaA, Weinheim

(MEK1/2) inhibitor (Calbiochem-Merck); other cells were co-treated with GDP-β-S (50 μM), a protein G inhibitor, or with Rottlerin (16 μM), a specific protein kinase C δ (PKCδ) inhibitor (Calbiochem-Merck). Because certain inhibitors were dissolved in DMSO, some cells were also treated with an equivalent volume of DMSO (14.1 mM) alone. Final concentrations of all chemical inhibitors were chosen as suggested by the relevant literature.

Incubation times for all experiments are in the figure legends.

2.5 RNA extraction

Total RNA was extracted from treated cells using TRIzol Reagent (Applied Biosystems, Monza, Italy) following the manufacturer's instructions. RNA was dissolved in RNase-free water fortified with RNase inhibitors (RNase SUPER-ase-In, Ambion, Austin, TX, USA). The amount and purity (A260/A280 ratio) of the extracted RNA were assessed spectrophotometrically.

2.6 cDNA preparation and real-time RT-PCR

cDNA was synthesized by reverse transcription from 2 μg RNA with a commercial kit and random primers (High-Capacity cDNA Reverse Transcription Kit, Applied Biosystems) following the manufacturer's instructions. Singleplex real-time RT-PCR was performed on 25 ng of cDNA using TaqMan Gene Expression Assay kits prepared for human CD36 and β_2-microglobulin, TaqMan Fast Universal PCR Master Mix, and 7500 Fast Real-Time PCR System (Applied Biosystems). Negative controls did not include RNA. The oligonucleotide sequences are not revealed by the manufacturer due to proprietary interests. The cycling parameters were as follows: 20 s at 95°C for AmpErase UNG activation, 3 s at 95°C for AmpliTaq Gold DNA polymerase activation, 40 cycles of 3 s at 95°C (melting) and 30 s at 60°C (annealing/extension). The fractional cycle number (Ct) at which fluorescence passes the threshold in the amplification plot of fluorescence signal *versus* cycle number was determined for each gene considered. The results were then normalized to the expression of β_2-microglobulin, as housekeeping gene. Relative quantification of target gene expression was achieved with a mathematical method proposed by Livak and Schmittgen [17].

2.7 siRNA transfection

siRNA was used for transient gene knockdown studies. Transfection of PKCδ, MEK1 and MEK2 specific and negative control siRNAs was carried out following the manufacturer's instructions (Ambion). The siRNAs used were PRCKD siRNA, MAP2K1 siRNA, MAP2K2 siRNA, GNA_Q siRNA, GNA_{13} siRNA, glyceraldehyde-3-phosphate dehydrogenase siRNA and negative control (scramble) siRNA (Ambion). Briefly, 50 nM of siRNAs were mixed with 25 μL of transfection reagent solution (NeoFX, Ambion) and left at room temperature for 10 min. After 24 h of reverse transfection, the cells (8×10^4/mL) were centrifuged and incubated with oxysterol mixture 20 μM for 6 h in replaced medium with 2% fetal bovine serum. For gene expression analysis, total RNA was isolated from the cells and used for quantitative RT-PCR as described above. The transfection efficiency, validated by quantitative RT-PCR, was approximately 60%.

2.8 Western blotting

Whole cell extracts were prepared in ice-cold lysing buffer (20 mM Hepes, pH 7.9, 0.35 M NaCl, 20% glycerol, 1% (octylphenoxy)polyethoxyethanol, 1 mM $MgCl_2$, 0.5 mM EDTA, 0.1 mM EGTA) containing protease inhibitors for 30 min, and the lysates were then cleared by centrifugation at 15 000 rpm for 15 min. The protein concentration was measured following Bradford's method [18].

To analyze the levels of phosphorylated extracellular signal-regulated kinase (pERK) total proteins (50 μg) were boiled for 5 min in Laemmli buffer and separated by electrophoresis in 10% denaturing SDS/polyacrylamide gel followed by transfer to Hybond ECL nitrocellulose membrane (GE Healthcare Europe, Milan, Italy). For pPKCδ level analysis, 100 μg of total proteins were immunoprecipitated with 8 μL of anti-PKCδ primary antibody (Santa Cruz Biotechnology, Santa Cruz, CA, USA), purified on Protein A Sepharose resin (GE Healthcare Europe), boiled in Laemmli buffer, separated by electrophoresis in 10% denaturing SDS/polyacrylamide gel, and then electroblotted onto nitrocellulose membrane. After saturation of non-specific binding sites with 5% non-fat milk in Tris-buffered saline 1X-Tween 20 0.05%, membranes were immunoblotted overnight at 4°C with the appropriate primary antibody against pPKCδ (1:250) or pERK1/2 (1:250) (Santa Cruz Biotechnology), diluted respectively in 5% non-fat milk or 1% BSA in Tris-buffered saline 1X-Tween 20 0.05% and subsequently probed with a specific horseradish peroxidase-conjugated secondary antibody (Santa Cruz Biotechnology). After stripping (Restore Western Blot Stripping buffer, Pierce Biotechnology, Rockford, IL, USA), membranes were again immunoblotted with anti-PKCδ (1:500) or anti-ERK1/2 (1:5000) primary antibody (Santa Cruz Biotechnology) and then incubated with an appropriate secondary antibody, as described above. Proteins detected by the antibodies were visualized through enhanced chemiluminescence using the ECL-plus kit (GE Healthcare Europe) following the manufacturer's protocol. The immunoreactive bands were scanned and subjected to densitometric analysis using the ''Image Tool'' software (Windows 3.00). The results were evaluated as relative units determined by normalization of the density of each band to that of the corresponding referred protein band.

© 2010 WILEY-VCH Verlag GmbH & Co. KGaA, Weinheim

2.9 Analysis of CD36 by confocal laser microscopy

Cells were transferred onto glass slides (10×10^4 cells/slide) by cytocentrifugation. The specimens were fixed in 95% ethanol and then incubated in a 100 mM sodium cyanoborohydride reducing agent. After blocking non-specific binding, the slides were incubated in the presence of mouse monoclonal antibodies to human CD36 (1:2000) (Clone FA6-152, HyCult biotechnology b.v.) or of peroxisome proliferator-activated receptor γ (PPARγ) (1:500) (Santa Cruz Biotechnology) and then with purified goat anti-mouse FITC fluorochrome-conjugated secondary antibodies (1:300) (Alexa Fluor 488, Molecular Probes-Invitrogen Srl). Slides mounted with MOWIOL 4–88 (Calbiochem-Merck) were observed through the LSM 510 confocal laser microscope (Carl Zeiss SpA).

2.10 Statistical analysis

All values are expressed as means ± SD. Statistical analysis of the data was assessed by using the one-way ANOVA with Bonferroni's post test for multiple comparisons and the *t* test with Welch correction for comparison between two groups. Differences with $p < 0.05$ were considered statistically significant. Statistical calculations were carried out with GraphPad InStat3 software (GraphPad Software, San Diego, CA, USA).

3 Results

3.1 Co-localization of CD68 cells, CD36 receptor and LDL in human atherosclerotic plaques

With the aim of directly checking the localization of cells of the macrophage lineage (CD68 positive cells), CD36 scavenger receptors and accumulated LDL particles in human atherosclerotic lesions, aliquots of human carotid plaques were used for immunohistochemical and immunofluorescent analyses. Immunohistochemistry performed on serial slices from the single plaques consistently showed good co-localization of CD68, specific marker of cells of the macrophage lineage, and CD36 scavenger receptor in the core region of the atheromas, within the sub-intimal space of the artery (Fig. 1). Detection of LDL apoprotein B100 by immunofluorescence showed these micelles to be particularly concentrated at the level of the plaque CD68/CD36 accumulation (Fig. 1). As expected, slice staining with Nile red, a lipid dye [19], confirmed the prevalent lipid accumu-

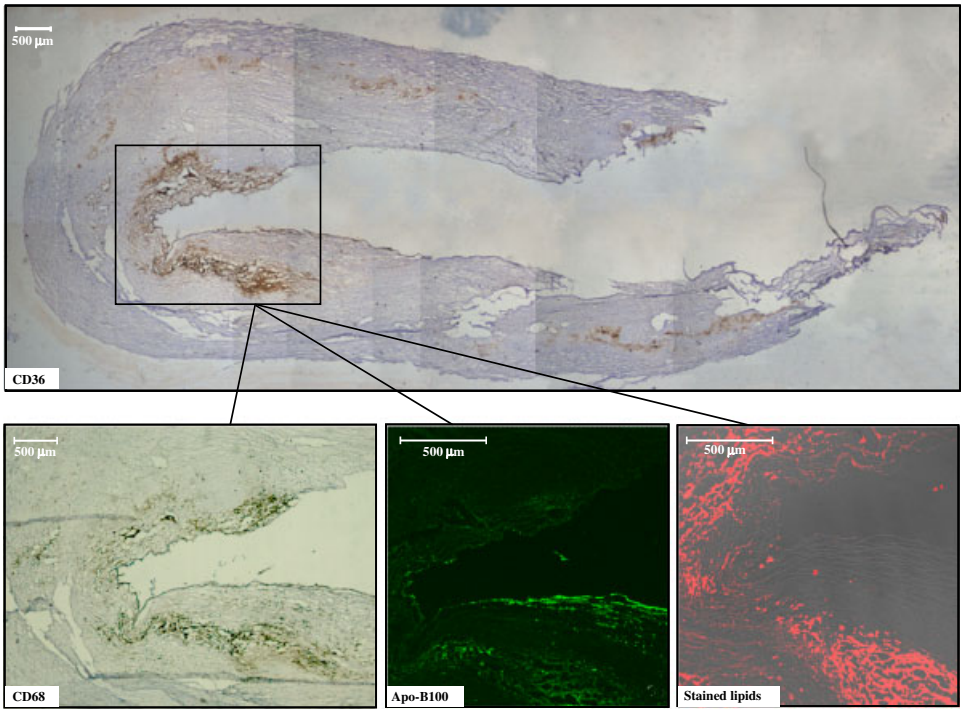

Figure 1. Plaque CD68/CD36 co-localization and LDL apoprotein B100 and lipids. The relative distribution of CD68 and CD36 in consecutive sections of the same carotid plaque was visualized by immunohistochemistry. Images, observed by light microscopy, were acquired with the ''Leica DCF Twain'' program (× 25). LDL apoprotein B100 (Apo-B100) and lipid material accumulated in sections of the same human carotid plaque were respectively observed by immunofluorescence or after Nile red staining. Images were observed by confocal laser microscopy (apoprotein B100: FITC fluorochrome-conjugated secondary antibodies, excitation from the 488 nm Ar laser line and emission passing through a long pass 505–550 filter, lens 5 × /0.15; lipid accumulation: Nile red staining, excitation from the 543 nm HeNe laser line and emission passing through a long pass 560 filter, lens 5 × /0.15, 2 ×). Images are from one representative plaque out of four.

© 2010 WILEY-VCH Verlag GmbH & Co. KGaA, Weinheim

lation in this region (Fig. 1). The tissue around the atherosclerotic lesion, apparently normal, did not show positivity for CD36. This result clearly underlines the involvement of the scavenger receptor CD36 in the atherosclerotic lesion progression. The observed data where confirmed in four other different plaques.

3.2 Involvement of G protein/Src/PLC cascade in the oxysterol mediated up-regulation of CD36 receptor levels on U937 promonocytic cells

Starting from the hypothesis that molecular signaling by oxysterols would likely involved G proteins and the PLC cascade, as was demonstrated many years ago for oxidized LDL [20–22], U937 cells were challenged with the same oxysterol mixture that had been shown to markedly up-regulate CD36 expression and synthesis [15], this time in the presence or absence of selective inhibitors of that pathway. As shown in Fig. 2, the marked induction of CD36 observed when U937 cell aliquots were incubated 48 h with the oxysterol mixture (20 μM) was completely prevented by cell co-incubation with GDP-β-S (50 μM), a widely used G protein inhibitor. The same result was obtained with 30 min cell pre-treatment with PP2 (2 μM), an inhibitor of tyrosine kinase c-Src, or with U73122 (2 μM), a PLC inhibitor; conversely, a close analogue of the latter compound, U73343, which does not inhibit PLC, did not modify the stimulating action of the oxysterol mixture on CD36 membrane levels at all (Fig. 2).

3.3 Enhanced phosphorylation of PKCδ in U937 cells induced by challenging the cells with the oxysterol mixture, but not with unoxidized cholesterol

The involvement of the PLC cascade in CD36 up-regulation by oxysterols suggested that the consequent production of phos-

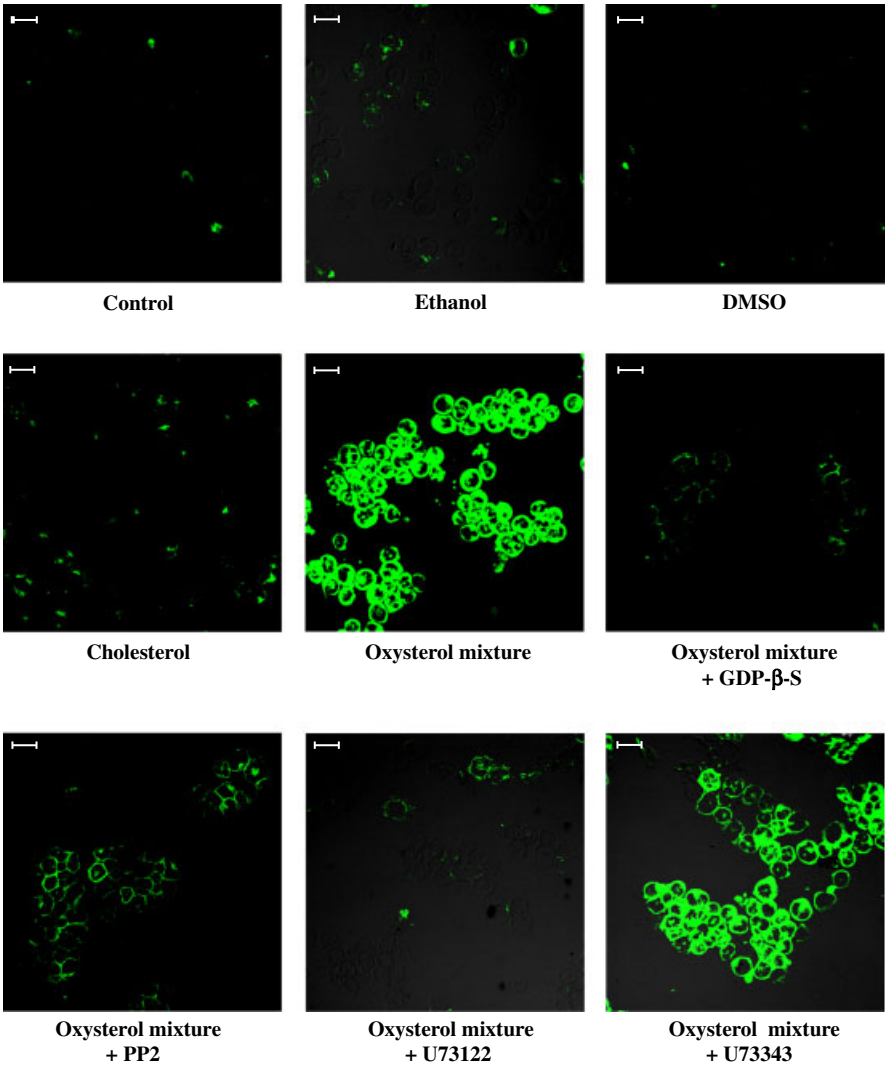

Figure 2. Involvement of the G protein/Src/PLC cascade in CD36 synthesis induced by the oxysterol mixture in cells of the macrophage lineage. U937 cells were incubated for 48 h with cholesterol (20 μM) or oxysterol mixture (20 μM). Untreated cells were used as control and cells supplemented with 12.5 mM ethanol or 14.1 mM DMSO as solvent controls. Cells were pre-treated with PP2 (2 μM) or U73122 (2 μM) or with the inactive analogue U73343 (2 μM). Other cells were co-treated with GDP-β-S (50 μM). CD36 protein levels were detected by confocal laser microscopy using FITC fluorochrome (excitation from the 488 nm Ar laser line and emission passing through a long pass 505–550 filter, lens 40 × /0.75). Images are from one representative experiment out of three. Bars: 20 μm.

© 2010 WILEY-VCH Verlag GmbH & Co. KGaA, Weinheim

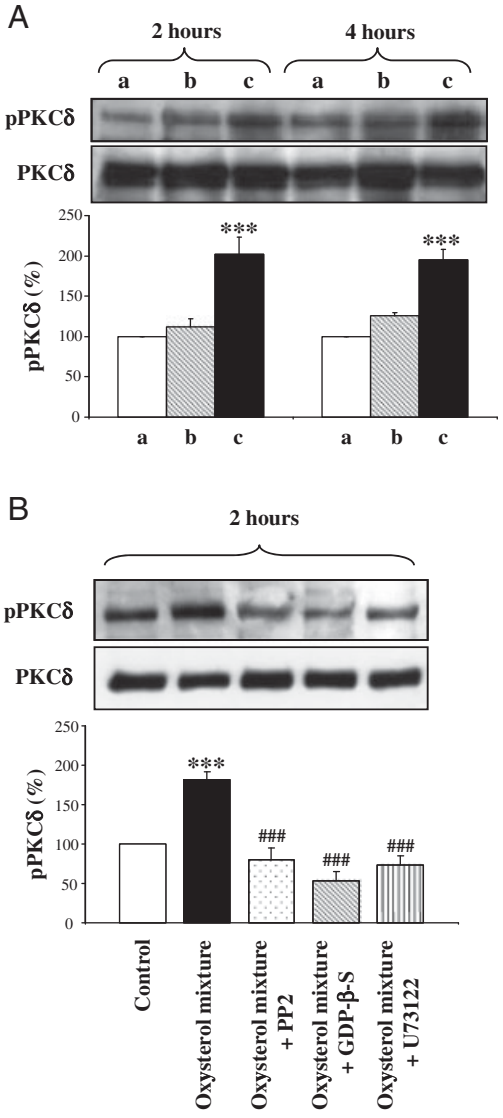

Figure 3. Induction and inhibition of PKCδ phosphorylation in U937 cells. (A) U937 cells were incubated with cholesterol (20 μM) or oxysterol mixture (20 μM) for 2 and 4 h. Cells incubated in the presence of solvent alone (12.5 mM) were used as internal control. PKCδ levels were analyzed by Western blotting as described in Section 2; the membranes were immunoblotted with polyclonal antibodies against pPKCδ and PKCδ. One blot representative of four experiments is shown. Histograms represent the mean values ± SD of all four independent experiments; pPKCδ densitometric measurements were normalized against the corresponding PKCδ levels and expressed as percentage of the solvent group. ***$p<0.001$ *versus* solvent a: Ethanol; b: Cholesterol; c: Oxysterol mixture. (B) U937 cells were incubated for 2 h with oxysterol mixture (20 μM). Cells were also pre-treated with PP2 (2 μM), or U73122 (2 μM) or co-treated with GDP-β-S (50 μM). Untreated cells were used as control. PKCδ levels were analyzed by Western blotting. One blot representative of three experiments is shown. Histograms represent the mean values ± SD of all experiments; pPKCδ densitometric measurements were normalized against the corresponding PKCδ levels and expressed as percentage of the control. ***$p<0.001$ *versus* control and ###$p<0.001$ *versus* oxysterol mixture.

phatidylinositol biphosphate and diacylglycerol would directly stimulate members of the PKC family. Indeed, the complete prevention of oxysterol-mediated CD36 receptor up-regulation in U937 cells with the well-known PKCδ inhibitor Rottlerin, reported elsewhere [15], suitably orientated to that specific cell signaling analysis. Focusing on the first few hours of cell incubation in the presence of the oxysterol mixture (20 μM), PKCδ phosphorylation, measured by Western blotting, was found to be about double that of cells incubated for 2 or 4 h in the presence of identical amounts of unoxidized cholesterol or

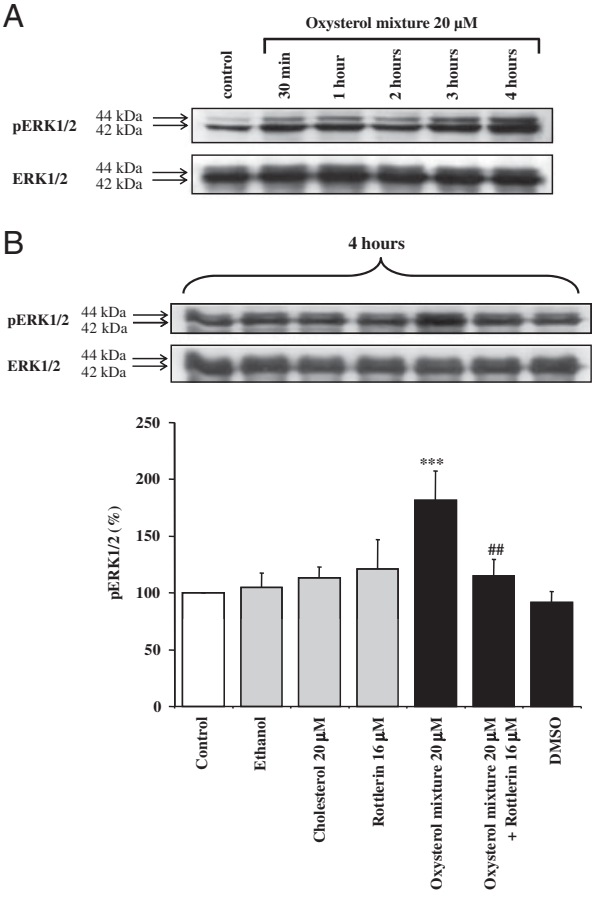

Figure 4. Implications of the ERK1/2 pathway and inhibition of ERK phosphorylation by Rottlerin, a selective inhibitor of PKCδ. (A) U937 cells were treated with the oxysterol mixture (20 μM) from 30 min up to 4 h. Untreated cells were used as control. Time-course levels of pERK1/2 were analyzed by Western blotting. One representative blot of two experiments is shown. (B) Cells were treated with the oxysterol mixture (20 μM) or cholesterol (20 μM) for 4 h. Other cells were co-treated with Rottlerin (16 μM) and the oxysterol mixture. Untreated cells were used as control and cells treated with ethanol (12.5 mM), DMSO (14.1 mM) or Rottlerin (16 μM) were taken as internal controls. Levels of pERK1/2 were analyzed by Western blotting. One representative blot is shown for phosphorylated and non-phosphorylated ERK1/2 levels. Histograms represent the mean values ± SD of pERK1/2 levels normalized against the corresponding ERK1/2 levels of three experiments and expressed as percentage of the control values. ***$p<0.001$ *versus* control and ##$p<0.01$ *versus* oxysterol mixture.

© 2010 WILEY-VCH Verlag GmbH & Co. KGaA, Weinheim

solvent alone (Fig. 3A). The link of G protein/Src/PLC cascade signaling with PKCδ phosphorylation induced by oxysterols was also observed using the selective chemical inhibitors of this pathway (Fig. 3B). The obtained data support the hypothesis that this signaling pathway is involved in oxysterol mixture-induced CD36 overexpression.

Following PKCδ phosphorylation, the involvement of ERK1/2 was clearly demonstrated by a time-dependent experiment with a maximum of ERK phosphorylation after 4 h of cell treatment with the oxysterol mixture (20 μM) (Fig. 4A). Importantly, by preventing the stimulating effect of the oxysterol mixture on PKCδ phosphorylation by U937 cell pre-treatment with Rottlerin (16 μM), phosphorylation of ERK1/2 was also inhibited (Fig. 4B).

3.4 Prevention of oxysterol-induced CD36 overexpression in U937 cells by cell transfection with $G\alpha_q$, $G\alpha_{13}$, PKCδ or MEK1/MEK2 siRNAs

In order to definitively demonstrate a crucial role for the PKCδ and MEK/ERK kinase pathways in up-regulating CD36 scavenger receptors in cells of the macrophage lineage (*i.e.* the molecular event necessary for these cells to be transformed into foam cells) U937 cells were first transfected with specific siRNAs (50 nM) then incubated for 6 h with the oxysterol mixture. Some cell aliquots were incubated in the absence of oxysterols, not transfected (internal control) or transfected with non-specific RNA sequences (negative control). Unlike wild-type cells that, after 6 h incubation with the oxysterol mixture, showed a 2.5–3 fold increase in CD36 mRNA, all cells transfected either with PKCδ siRNA (Fig. 5B) or with MEK1 and MEK2 siRNAs (Fig. 5C) exhibited a mRNA for the scavenger receptor that was quantitatively similar, though not identical, to that of the negative and internal controls. To check the involvement of G proteins in CD36 overexpression, other cells were transfected with $G\alpha_q$, $G\alpha_{13}$ siRNAs; the levels of the scavenger receptor mRNA was, in both cases, significantly decreased comparing to oxysterol mixture-treated cells (Fig. 5A). Demonstration of a good knockdown efficiency of the used siRNAs is shown in Fig. 5D.

3.5 Induction of the transcription factor PPARγ as oxysterol-signaling downstream of ERK

The role played by PPARγ [23] in the regulation of CD36 expression is well known. With the aim of clarifying oxysterol-

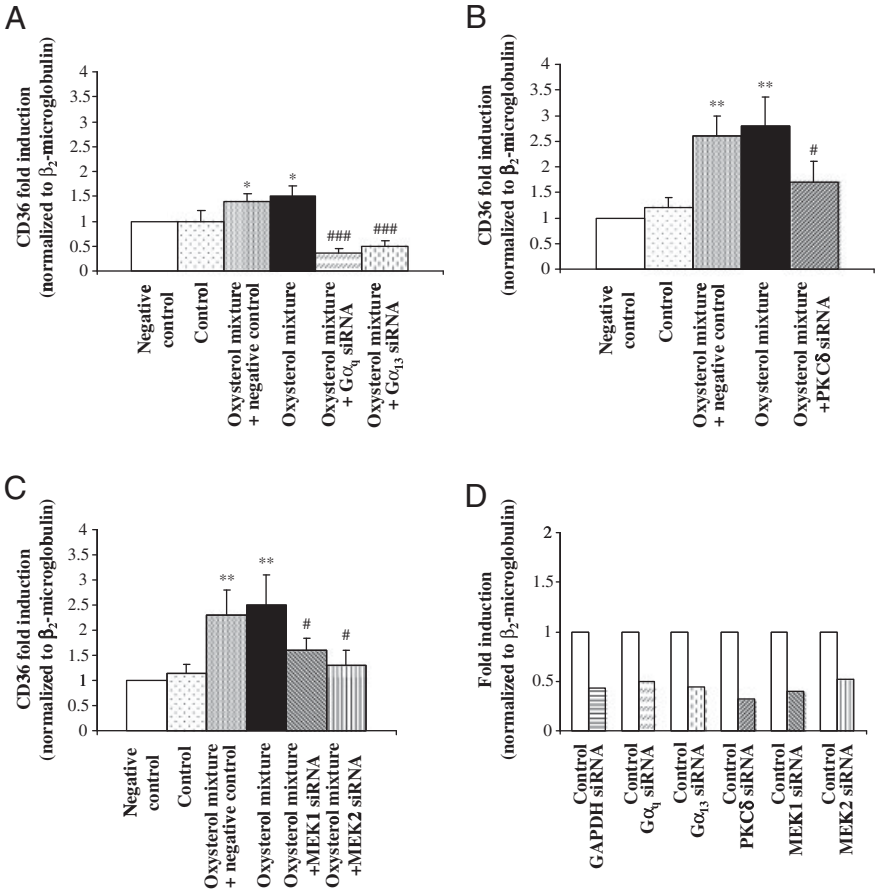

Figure 5. Prevention of oxysterol-induced CD36 overexpression by G proteins, PKCδ or MEK1/MEK2 siRNAs. Verification of $G\alpha_q$ and $G\alpha_{13}$ (A), PKCδ (B) or MEK1/MEK2 (C) specific siRNAs (50 nM) on expression of CD36 in U937 cells treated with the oxysterol mixture (20 μM) for 6 h after reverse transfection (24 h). Untreated cells were used as control and cells transfected with not specific siRNA as negative control (scramble). Expression of the CD36 gene was quantified by real time RT-PCR. Data, normalized to β_2-microglobulin, are expressed as mean values ± SD of three experiments. $^{**}p<0.01$ and $^{*}p<0.05$ *versus* negative control; $^{\#\#\#}p<0.001$ and $^{\#}p<0.05$ *versus* oxysterol mixture group. (D) Knockdown efficiency of the used siRNAs. Glyceraldehyde-3-phosphate dehydrogenase siRNA was used as positive control.

© 2010 WILEY-VCH Verlag GmbH & Co. KGaA, Weinheim

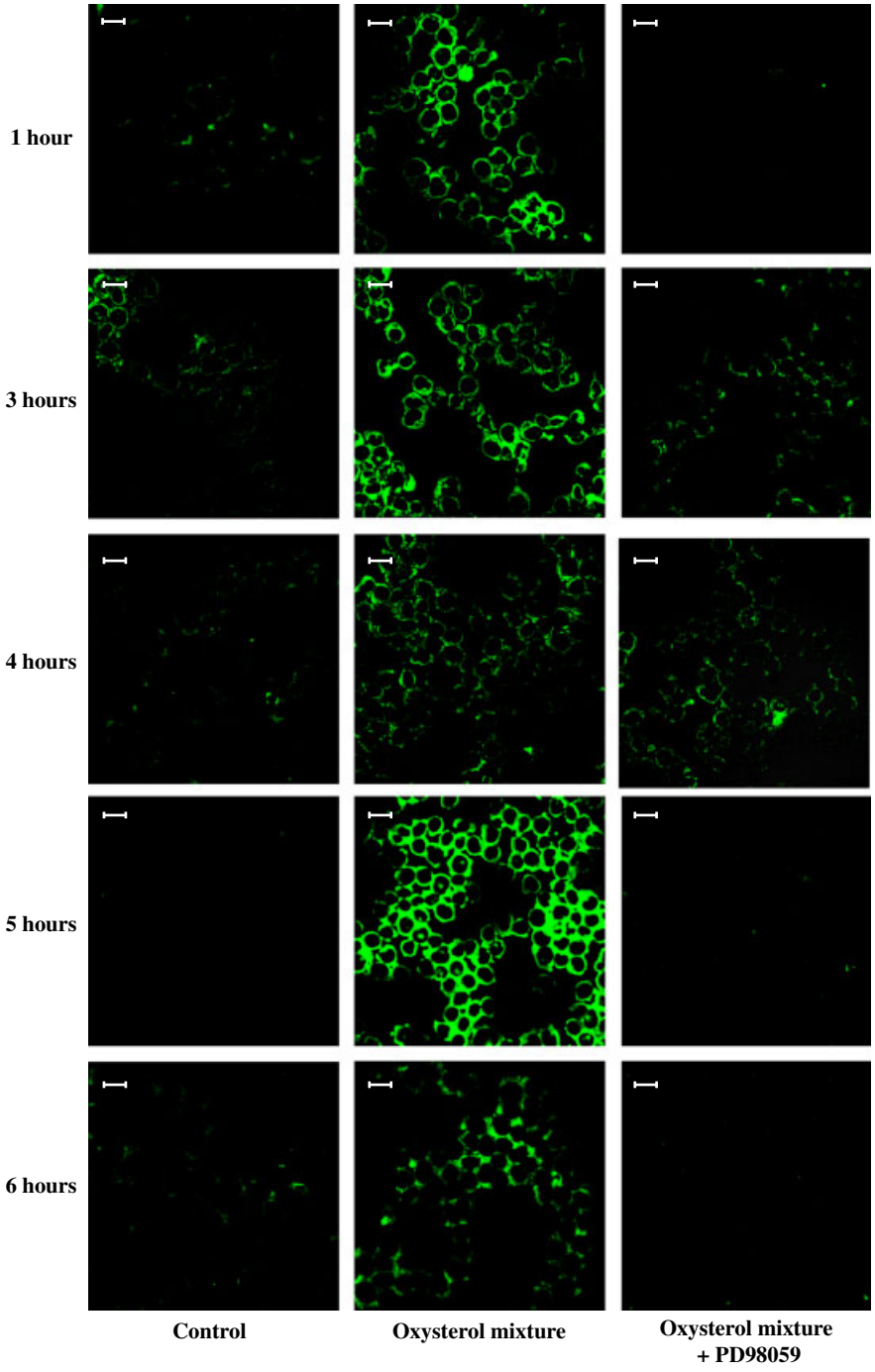

Figure 6. Inhibition of ERK1/2 by PD98059, a selective inhibitor of the upstream MEK1/2, reduces PPARγ up-regulation. After 30 min pre-incubation with PD98059 (20 μM), cells were incubated up to 6 h with the oxysterol mixture (20 μM). PPARγ levels were visualized by confocal laser microscopy using FITC fluorochrome (excitation from the 488 nm Ar laser line and emission passing through a long pass 505–550 filter, lens 40 × /0.75). Images are from one representative experiment out of three. Bars: 20 μm.

signaling downstream of ERK1/2, such as PPARγ, the cells were pre-treated with PD98059, a selective inhibitor of MEK1/2, and then with the oxysterol mixture (20 μM) for intervals ranging from 1 to 6 h. PPARγ was consistently induced by the oxysterols with a maximum after 5 h treatment, and the likely connection between MEK/ERK and this transcription factor was observed when the cells were pre-incubated with PD98059. PPARγ up-regulation was markedly reduced by inhibiting ERK phosphorylation (Fig. 6).

4 Discussion

This article reports evidence of a significant overexpression of CD36 receptor on cells of the macrophage lineage, *i.e.*

© 2010 WILEY-VCH Verlag GmbH & Co. KGaA, Weinheim

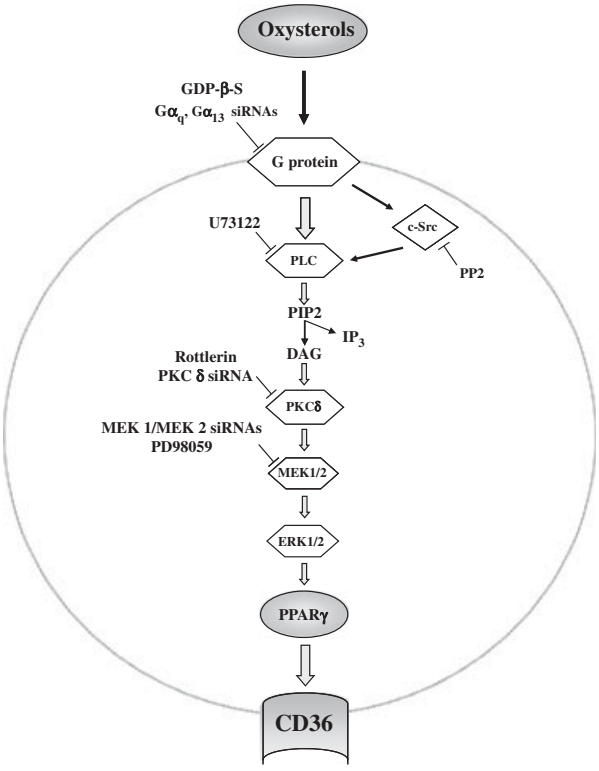

Figure 7. Schematic representation of a hypothetical model for the signaling pathway involved in oxysterol mixture-induced CD36 overexpression.

CD68 positive cells, which co-localized with the accumulation of LDL apoprotein B100 and lipids in human advanced atherosclerotic lesions (Fig. 1). The observation that all these proteins are increased in atherosclerotic human carotid lesions compared with normal areas are reported by other authors confirming their role in the pathology of atherosclerosis [24, 25]. Moreover, a significant close correlation has recently been observed between the total oxysterols recovered from advanced atherosclerotic lesions in the human carotid, and the respective total cholesterol, both being measured by gas chromatography on plaque homogenate [7]. This implies that in advanced lesions, which are characterized by the presence of several cells of the macrophage lineage, *i.e.* CD68 positive cells (Fig. 1), the more cholesterol accumulates, the higher is the production of oxysterols. However, while this is very interesting *per se*, a purely quantitative determination does not take into account that LDL cholesterol and derived oxidation products actually localize in discrete areas of the atherosclerotic lesion where foam cells tend to accumulate, *i.e.* in the core of the lesion (Fig. 1). Consequently, the actual concentration of accumulated oxysterols in an advanced atheroma might be considerably higher than that indicated by quantitative measurements made on aliquots taken from a plaque's homogenate (0.2–0.5 μmol/g wet weight tissue) [26]. Based on all these findings and considerations, *in vitro* investigations of biochemical features of oxysterols appear biocompatible only when using concentrations of single cholesterol oxides within the low micromolar range.

The increasing interest in the potential contribution of oxysterols to the pathogenesis of hypercholesterolemia-linked human diseases, in primis atherosclerosis, has over recent years generated a considerable bulk of evidence, which outlines the strong pro-apoptotic and pro-inflammatory activities of this class of compounds [7, 10, 26]. While most of the relevant experimental studies employed single cholesterol oxidation products, a few considered mixtures of oxysterols that are present in oxidized dietary lipids, circulating lipoproteins and atherosclerotic lesions [27, 28]. The experiments reported here followed the very recent evidence of a marked up-regulation of the key scavenger receptor CD36 on macrophage cells (U937 cell line) *in vitro* challenged with a biologically compatible mixture of oxysterols [15].

As anticipated in the Introduction, the incubation of oxysterol-treated U937 cells in the presence of anti-CD36 specific antibodies stopped the formation of foam cells [15]. Because of this central role played by oxysterol-induced CD36 in the genesis of the atherosclerotic lesion, a basic depiction of the relevant signaling cascade (Fig. 7) appears important to provide new molecular insights into the mechanisms of atheroma formation, for further development of both preventative and therapeutic strategies.

The findings obtained by employing selective molecular inhibitors clearly pointed to the involvement of G proteins, of c-Src and of PLC cascade in the oxysterol-mediated signaling that leads to a net increase of CD36 on macrophagic cells (Fig. 2). According to the literature, using specific siRNAs, we demonstrated the involvement of the $G\alpha_q$ protein and of the $G\alpha_{13}$ protein upstream of PKC in CD36 overexpression (Fig. 5A).

PKC phosphorylation was recently reported to be crucial in oxysterol-induced osteoblastic differentiation of mesenchymal cells on the basis of the strong inhibitory effect exerted by Rottlerin, inhibitor of PKC novel isoforms and bisindolylmaleimide, inhibitor of both classic and novel isoforms [29]. In the present report, direct evidence of increased PKCδ phosphorylation was provided by Western blotting in U937 cells challenged with an oxysterol mixture (Fig. 3A) of a concentration and a relative composition compatible with those detectable in oxidized foodstuff and lipoproteins [8, 26]. A decrease of PKCδ phosphorylation was observed after the cell pre- or co-treatment with chemical inhibitors of G proteins/c-Src/PLCs (Fig. 3B). At present, this is the only available insight into oxysterols' signaling upstream of PKC.

Importantly, a conclusive demonstration of a primary role of PKCδ phosphorylation pathway in oxysterol-mediated CD36 overexpression was provided by the almost complete prevention of the latter event when macrophage cells were transfected with the siRNA specific for that novel PKC isoform (Fig. 5B). Moreover, inhibition of PKCδ

© 2010 WILEY-VCH Verlag GmbH & Co. KGaA, Weinheim

phosphorylation by cell co-treatment with Rottlerin prevented the induction of ERK1/2 phosphorylation pathway, induced by the same oxysterol mixture (Fig. 4B). Once again, siRNA experiments allowed us to conclusively demonstrate that MEK/ERK signaling also plays a key role, downstream of PKCδ, in the consistently observed oxysterol-dependent CD36 overexpression (Fig. 5C). Finally, induction of PPARγ by oxysterols was markedly reduced in cells pre-treated with PD98059, a selective inhibitor of MEK1/2, underlining the connection between the ERK and the PPARγ pathways (Fig. 6).

In conclusion, an oxysterol mixture compatible with that detectable in human hypercholesterolemic plasma, and including all major oxysterols of dietary origin, has shown the ability, in U937 cells of the macrophage lineage, to strongly up-regulate the CD36 scavenger receptor, by sustaining a molecular signaling that involves first G proteins-driven PLC cascade, then the PKC isoform δ and MEK/ERK phosphorylation and PPARγ pathways. In this way, cholesterol oxidation products of dietary origin, but not unoxidized cholesterol, could significantly contribute to foam cell formation in the developing atheromasic lesions, and consequently may aggravate the atherosclerotic disease process.

Very recently, the important role of dietary cholesterol in promoting macrophage accumulation in adipose tissue and the arterial wall has been reviewed, and strongly reaffirmed [30]. Oxysterols are most likely responsible for such a cholesterol-induced macrophage accumulation, because of their recognized ability to induce the production of at least monocyte chemotactic protein-1 [14] and interleukin-8 [31], two potent chemoattractants of cells of the macrophage lineage.

Thus, because of the strong pro-oxidant and pro-inflammatory potential of oxysterols, uncontrolled or quantitatively relevant oxidation of dietary cholesterol during food storage and processing may significantly sustain the expression of various human diseases. In particular, besides atherosclerosis, oxidized lipid products ingested in the diet could contribute to the promotion and progression of disease processes often associated with hypercholesterolemia, like inflammatory bowel diseases and colon cancer [32–34].

The authors wish to thank the European Science Foundation COST B35 Action, the Italian Ministry of University, PRIN 2006, the Region of Piedmont (Ricerca Sanitaria Finalizzata, 2006, 2007, 2008a, 2008b) and the University of Turin, Italy, for research support.

The authors have declared no conflict of interest.

5 References

[1] Stampfer, M. J., Hu, F. B., Manson, J. E., Rimm, E. B., Willett, W. C., Primary prevention of coronary heart disease in women through diet and lifestyle. *N. Engl. J. Med.* 2000, *343*, 6–22.

[2] Lichtenstein, A. H., Appel, L. J., Brands, M., Diet and lifestyle recommendations revision 2006: a scientific statement from the American heart association nutrition committee. *Circulation* 2006, *114*, 82–96.

[3] Steinberg, D., Atherogenesis in perspective: Hypercholesterolemia and inflammation as partners in crime. *Nature* 2002, *8*, 1211–1217.

[4] Leonarduzzi, G., Sottero, B., Poli, G., Oxidized products of cholesterol: dietary and metabolic origin, and proatherosclerotic effects. *J. Nutr. Biochem.* 2002, *13*, 700–710.

[5] Leonarduzzi, G., Chiarpotto, E., Biasi, F., Poli, G., 4-Hydroxynonenal and cholesterol oxidation products in atherosclerosis. *Mol. Nutr. Food Res.* 2005, *49*, 1044–1049.

[6] Staprans, I., Pan, X.-M., Rapp, J. H., Feingold, K. R., The role of dietary oxidized cholesterol and oxidized fatty acids in the development of atherosclerosis. *Mol. Nutr. Food Res.* 2005, *49*, 1075–1082.

[7] Poli, G., Sottero, B., Gargiulo, S., Leonarduzzi, G., Cholesterol oxidation products in the vascular remodeling due to atherosclerosis. *Mol. Aspects Med.* 2009, *30*, 180–189.

[8] Pie, J. E., Spahis, K., Seillan, C., Evaluation of oxidative degradation of cholesterol in food and food ingredients: identification and quantification of cholesterol oxides. *J. Agric. Food Chem.* 1990, *38*, 973–979.

[9] Dionisi, F., Golay, P. A., Aeschlimann, J. M., Fay, L. B., Determination of cholesterol oxidation products in milk powders: methods comparison and validation. *J. Agric. Food. Chem.* 1998, *46*, 2227–2233.

[10] Leonarduzzi, G., Sottero, B., Verde, V., Poli, G., in: Preedy, V. R., Watson, R. R. (Eds.), *Reviews in Food and Nutrition Toxicity*, CRC Press, Boca Raton 2005, pp. 129–164.

[11] Hennig, B., Toborek, M., Nutrition and endothelial function: implications in atherosclerosis. *Nutr. Res.* 2001, *21*, 279–283.

[12] Vejux, A., Lizard, G., Cytotoxic effects of oxysterols associated with human diseases: Induction of cell death (apoptosis and/or oncosis), oxidative and inflammatory activities, and phospholipidosis. *Mol. Aspects Med.* 2009, *30*, 153–170.

[13] Leonarduzzi, G., Sevanian, A., Sottero, B., Arkan, M. C. *et al.*, Up-regulation of the fibrogenic cytokine TGF-β1 by oxysterols: a mechanistic link between cholesterol and atherosclerosis. *FASEB J.* 2001, *15*, 1619–1621.

[14] Leonarduzzi, G., Gamba, P., Sottero, B., Kadl, A. *et al.*, Oxysterol-induced up-regulation of MCP-1 expression and synthesis in macrophage cells. *Free Radic. Biol. Med.* 2005, *39*, 1152–1161.

[15] Leonarduzzi, G., Gamba, P., Gargiulo, S., Sottero, B. *et al.*, Oxidation as a crucial reaction for cholesterol to induce tissue degeneration: CD36 overexpression in human promonocytic cells treated with a biologically relevant oxysterol mixture. *Aging Cell* 2008, *7*, 375–382.

[16] Febbraio, M., Podrez, E. A., Smith, J. D., Hajjar, D. P. *et al.*, Targeted disruption of the class B scavenger receptor CD36 protects against atherosclerotic lesion development in mice. *J. Clin. Invest.* 2000, *105*, 1049–1056.

© 2010 WILEY-VCH Verlag GmbH & Co. KGaA, Weinheim

[17] Livak, K. J., Schmittgen, T. D., Analysis of relative gene expression data using real-time quantitative PCR and the 2(-Delta Delta C(T)) method. *Methods* 2001, *25*, 402–408.

[18] Bradford, M. M., A rapid and sensitive method for the quantitation of microgram quantities of protein utilizing the principle of protein-dye binding. *Anal. Biochem.* 1976, *72*, 248–254.

[19] Klinkner, A. M., Bugelski, P. J., Waites, R., Louden, C. *et al.*, A novel technique for mapping the lipid composition of atherosclerotic fatty streaks by en face fluorescence microscopy. *J. Histochem. Cytochem.* 1997, *45*, 743–753.

[20] Resink, T. J., Tkachuk, V. A., Bernhardt, J., Bühle, F. R., Oxidized low density lipoproteins stimulate phosphoinositide turnover in cultured vascular smooth muscle cells. *Arterioscler. Thromb.* 1992, *12*, 278–285.

[21] Gutkind, J. S., The pathways connecting G protein-coupled receptors to the nucleus through divergent mitogen-activated protein kinase cascades. *J. Biol. Chem.* 1998, *273*, 1839–1842.

[22] Luttrell, L. M., Daaka, Y., Lefkowitz, R. J., Regulation of tyrosine kinase cascades by G-protein-coupled receptors. *Curr. Opin. Cell. Biol.* 1999, *11*, 177–183.

[23] Nicholson, A. C., Hajjar, D. P., CD36, oxidized LDL and PPARγ: pathological interactions in macrophages and atherosclerosis. *Vascul. Pharmacol.* 2004, *41*, 139–146.

[24] Nishi, K., Itabe, H., Uno, M., Kitazato, K.T. *et al.*, Oxidized LDL in carotid plaques and plasma associates with plaque instability. *Arterioscler. Thromb. Vasc. Biol.* 2002, *22*, 1649–1654.

[25] Collot-Teixeira, S., Barbatis, C., Bultelle, F., Koutouzis, M. *et al.*, CD36 is significantly correlated with adipophilin in human carotid lesions and inversely correlated with plasma ApoAI. *J. Biomed. Biotechnol.* 2008, *2008*, 813236.

[26] Leonarduzzi, G., Poli, G., Sottero, B., Biasi, F., Activation of the mitochondrial pathway of apoptosis by oxysterols. *Front. Biosci.* 2007, *12*, 791–799.

[27] Biasi, F., Leonarduzzi, G., Vizio, B., Zanetti, D. *et al.*, Oxysterol mixtures prevent proapoptotic effects of 7-ketocholesterol in macrophages: implications for proatherogenic gene modulation. *FASEB J.* 2004, *18*, 693–695.

[28] Larsson, D. A., Baird, S., Nyhalah, J. D., Yuan, X. M., Li, W., Oxysterol mixture, in atheroma-relevant proportions, display synergistic and proapoptotic effects. *Free Radic. Biol. Med.* 2006, *41*, 902–910.

[29] Richardson, J. A., Amantea, C. M., Kianmahd, B., Tetradis, S. *et al.*, Oxysterol-induced osteoblastic differentiation of pluripotent mesenchymal cells is mediated through a PKC- and PKA-dependent pathway. *J. Cell. Biochem.* 2007, *100*, 1131–1145.

[30] Subramanian, S., Chait, A., The effect of dietary cholesterol on macrophage accumulation in adipose tissue: implication for systemic inflammation and atherosclerosis. *Curr. Opin. Lipidol.* 2009, *20*, 39–44.

[31] Liu, Y., Hultén, L. M., Wiklund, O., Macrophages isolated from human atherosclerotic plaques produce IL-8, and oxysterols may have a regulatory function for IL-8 production. *Arterioscler. Thromb. Vasc. Biol.* 1997, *17*, 317–323.

[32] Chiarpotto, E., Scavazza, A., Leonarduzzi, G., Camandola, S. *et al.*, Oxidative damage and transforming growth factor β1 expression in pretumoral and tumoral lesions of human intestine. *Free Radic. Biol. Med.* 1997, *22*, 889–894.

[33] Biasi, F., Tessitore, L., Zanetti, D., Cutrin, J. C. *et al.*, Associated changes of lipid peroxidation and transforming growth factor β1 levels in human colon cancer during tumour progression. *Gut* 2002, *50*, 361–367.

[34] Zanetti, D., Poli, G., Vizio, B., Zingaro, B., 4-Hydroxynonenal and transforming growth factor-β1 expression in colon cancer. *Mol. Aspects Med.* 2003, *24*, 273–280.

© 2010 WILEY-VCH Verlag GmbH & Co. KGaA, Weinheim